

Single-vehicle data of highway traffic - a statistical analysis

L. Neubert¹, L. Santen^{1,2}, A. Schadschneider², M. Schreckenberg¹

¹ *Theoretische Physik/FB 10, Gerhard-Mercator-Universität Duisburg, D-47048 Duisburg, Germany,*
email: `neubert,santen,schreck@traffic.uni-duisburg.de`

² *Institut für Theoretische Physik, Universität zu Köln, D-50937 Köln, Germany, email: `as,santen@thp.uni-koeln.de`*
(March 13, 2018)

In the present paper single-vehicle data of highway traffic are analyzed in great detail. By using the single-vehicle data directly empirical time-headway distributions and speed-distance relations can be established. Both quantities yield relevant information about the microscopic states. Several fundamental diagrams are also presented, which are based on time-averaged quantities and compared with earlier empirical investigations. In the remaining part time-series analyses of the averaged as well as the single-vehicle data are carried out. The results will be used in order to propose objective criteria for an identification of the different traffic states, e.g. synchronized traffic.

I. INTRODUCTION

Experimental and theoretical investigations of traffic flow are focus of extensive research interest during the past decades [1–5]. Various theoretical concepts (e.g. [6–10]) have been developed and numerous empirical observations have been reported [11–15]. Despite these enormous scientific efforts both theoretical concepts as well as experimental findings are still under debate. In particular the empirical analysis turns out to be very subtle because the data strongly depend on several external influences, e.g. weather conditions, or the performance of junctions [12]. Therefore, even certain experimental facts are not well established, although considerable progress has been made in the past few years. To date, the following experimental view of highway traffic seems to be of common knowledge and generally accepted: It has been found that at least three states with qualitatively different behavior exist, namely free-flow, stop-and-go and synchronized states [11,13–15]. In addition to the existence of qualitative different phases some other interesting phenomena have been observed, e.g. the spontaneous formation of jams [16], and hysteresis effects [12].

This work focuses basically on two points. First of all we present a *direct analysis of single-vehicle* data which leads to a more detailed characterization of the different microscopic states of traffic flow, and second we use standard techniques of time-series analysis in order establish *objective* criteria for an identification of the different states.

A more detailed characterization of the microscopic structure of the different traffic states should lead to sensitive checks of the different modeling approaches. In particular the time-headway distributions and the speed-distance relations, which, to our knowledge for the first time, have been calculated from the single-vehicle data, allow for a quantitative comparison with simulation results of microscopic models [17–19]. Moreover the objective criteria for an identification of the different traffic states, developed in the framework of this article, allow for an unbiased analysis of the experimental data.

The paper is organized as follows. In section II we present some technical details of the measurements as

well as of the given data set. The analysis of single-vehicle data is presented in section III. Explicitly we show results for the time-headway distribution and the speed-distance relations. These results are compared to earlier estimates based on data from Japanese highways [11,10]. In section IV we show the results for the fundamental diagram. Here we focus on the effect of different time-intervals for the collection of data and discuss different methods for the calculation of the stationary fundamental diagram. Finally the time-series analysis of the single-vehicle data as well as of the aggregated data are presented in section V.

II. REMARKS ON THE DATA-COLLECTION

The data set is provided by 12 counting loops all located at the German highway A1 near Cologne. At this section of the highway a speed limit of 100 km/h is valid – theoretically.

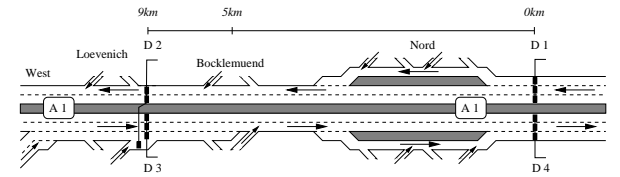


FIG. 1. Sketch of the analyzed section of the German highway A1. The driving directions are given by the arrows. The detector pairs D1/D4 and D2/D3 are about 9 km apart, in between a additional junction is located.

In Fig. 1 the section of the highway and the position of the detectors are sketched. A detector consists of three individual detection devices, one for each lane. By combining three devices covering the three lanes belonging to one direction (except D2, see Fig. 1) one gets the cross-section labeled D1 through D4. The two detector arrangements D1 and D4 are installed at the intersection of two highways (AK Köln-Nord), while D2 and D3 are located close to a junction (AS Köln-Lövenich).

These locations are approximately 9 km apart. In between there is a further junction but with a rather low usage. The most interesting results are obtained at D1 where the number of lanes is reduced from three to two for cars passing the intersection towards Köln-Lövenich. Therefore, this part of the highway effectively acts as a bottleneck. Consequently, congested traffic is most often recorded at detector D1, and the analysis is mainly based on this data set.

The data were collected between June 6, 1996 and June 17, 1996 when a total number of more than 500,000 vehicles passed each cross-section, with a portion of trucks and trailers of about 16% on average. During this period the traffic data set was not biased due to road constructions or bad weather conditions.

The distance-headway Δx as well as the velocity v of the vehicles passing a detector are collected in the data set. The velocity v is derived from the time elapsed between the crossing of the first and the second detector installed in a row with a known distance (usually 2 m). The second direct measure is the time elapsed between two consecutive vehicles. Due to storage capacity reasons it is saved with a rough resolution (only 1 sec), but used to determine the distance between the vehicle $n + 1$ and its predecessor n via* $\Delta x_{n+1} = v_n \Delta t_{n+1}$. It should be mentioned that this procedure gives correct results as far as the velocity *at* the detector is constant. Here the small spatial extension of the detectors guarantees that this assumption is fulfilled. So it is admissible to overcome the restriction of the resolution applying the reverse procedure to recover Δt with higher accuracy as it has been used in the framework of this paper.

For a sensible discussion it is plausible to split up the data set according to the different traffic states. In Fig. 2 a typical time-series of one minute aggregates of the speeds at the detectors D1 and D2 is shown. The transition from a free-flow to a congested state is indicated by a sudden drop of the local velocity. This allows for an undoubted separation of the data set into free-flow and congested regimes. Then the analysis of the data has been performed separately for the free-flow and congested states excluding the transition regime. At D1, the most interesting installation, one obtains eight different periods of both free-flow and congested states. These periods are labeled by numbers I through VIII.

Fig. 2 also shows the bottleneck-effect given by the lane-reduction near the intersection. At D1, the cross-section behind the local defect, one gets a sudden drop in the velocity. On the other hand, downstream this cross-section one finds only a weak decay of the velocity which represents the outflow from a jam.

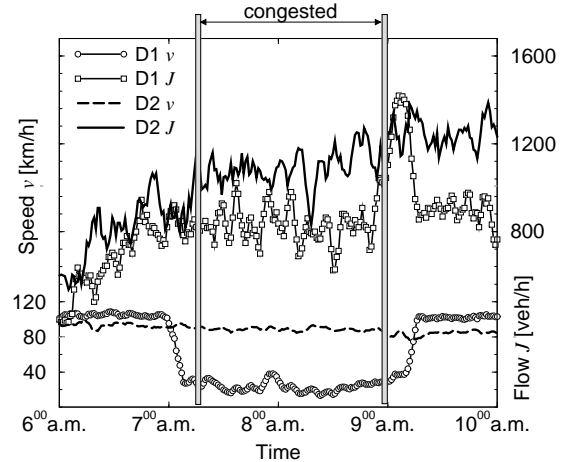


FIG. 2. Typical time series of flow and velocity. The transition from free to congested flow is indicated by a sharp fall of the average velocity. Upstream the bottleneck one finds a strong reduction of the speed at D1, whereas the flow remains nearly constant. Downstream the bottleneck at D2 the outflow from a jam is recorded – the speed is almost constant. It increases again after the jam at D1 has dissolved. For a proper characterization of the different states we excluded the transition region, e.g. for the shown realization of a congested we restricted our analysis on the part of the time-series between the two vertical lines.

III. ANALYSIS OF SINGLE-VEHICLE DATA

In this section the results for the time-headway distributions and speed-distance relations calculated from single-vehicle data are presented. For a detailed examination the data set was classified in two ways. As mentioned above a discrimination between free-flow and congested states was made, followed by a classification due to local densities[†]. Whereas the first one was done by a simple and manual separation by means of the time series of the speed, the second one requires a more detailed explanation: Every count belongs to a certain minute, and the local density ρ obtained during this certain minute is the criterion for the classification. I.e., it is conceivable that a distance-headway Δx is much larger than the mean distance-headway $\langle \Delta x \rangle \propto \rho^{-1}$ of the considered period. Moreover, for the analyses made in this section the traffic states recognized as stop-and-go traffic are omitted, since the determination of the related local densities strongly depends on the used method[‡]. So only the synchronized

*This implies that the error in calculating Δx_{n+1} increases with Δt_{n+1} , since the calculation is made under the assumption of a constant speed v_n .

[†]In Appendix A it is described how the local density is deduced from the data set.

[‡]This inevitable behavior of the local density is more precisely discussed in Appendix A. Stop-and-go traffic is charac-

states remain.

A. Time-headway distribution

In section II the way of calculating the time-headways Δt is described in detail. In principle the accuracy of the measurement would allow for a very fine resolution of the time-headway distribution, but in order to obtain a reliable statistics we have chosen time-intervals of length 0.1 sec. In Fig. 3 the time-headway distributions of different traffic states at different local densities ρ are displayed. Regardless of the value of the local density

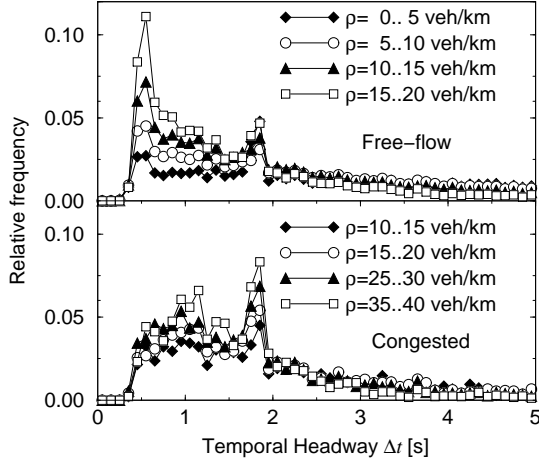


FIG. 3. Time-headway distribution for different density regimes. Top: In free-flow states the Δt -distribution is dominated by two peaks at 0.8 sec and 1.8 sec. Bottom: This diagram concerns congested states, the peak at 1.8 sec remains. In both cases there is a significant share of vehicles with $\Delta t < 1$ sec.

all free-flow distributions are dominated by a two-peak structure. The first peak at $\Delta t = 0.8$ sec represents the global maximum of the distribution and is in the range of time a driver typically needs to react to external incidents.

On a microscopic level this short time-headways correspond to platoons of some vehicles traveling very fast – their drivers are taking the risk of driving “bumper-to-bumper” with a rather high speed. These platoons are the reason for the occurrence of high-flow states in free traffic. The corresponding states exhibit meta stability, i.e. a perturbation of finite magnitude and duration is able to destroy such a high-flow state [20]. Once such

a collapse of the flow resp. the speed emerges, the free-flow branch can only be reached again by reducing the local density [20,21]. In the data base considered here such a sharp fall is not observable since all detected jams are caused by the bottleneck downstream the detector D1. Additionally, a second peak emerges at $\Delta t = 1.8$ sec which can be associated with a typical drivers’ behavior: It is recommended and safe to drive with a temporal distance of ≈ 2 sec corresponding to a maximum flow of $\approx 1,800$ veh/h.

Surprisingly, the small time-headways have much less weight in congested traffic but the peak at $\Delta t = 1.8$ sec is recovered. Here the background signal is of greater importance. The observed peak corresponds to the typical temporal headway (≈ 2 sec) of two vehicles leaving a jam consecutively.

However, almost every fourth driver falls below the 1-sec-threshold, and this is more likely when the traffic is free-flowing. Moreover, our results indicate that the small time-headways are of the highest weight in the transition regime between free-flow and congested flow.

The common structure of the time-headway distributions in all density regimes can be summarized as follows: A background signal covers a wide range of temporal headways, especially for $\tau < 1$ sec. Additionally, at least one peak is to be noticed.

B. Speed distance-headway characteristics

Probably the most important information for an adjustment of the speed is the accessible distance-headway Δx . This is captured by several models which use either a stationary fundamental diagram [22] or even more directly a so-called optimal-velocity (OV-) function $v = v(\Delta x)$ as input parameters [10]. Therefore, a detailed analysis of the speed-distance relationship is of great importance for the modeling of traffic flow. By means of Fig. 4 it is obvious that the average speed does not only depend on Δx itself, but also on the local density. In particular, the average speed for large distances in congested states is significantly lower than for the free flow states, but also saturated for sufficiently large Δx . Next we also took into account the velocity differences $\Delta v = v_n - v_{n+1}$ between consecutive cars (n followed by $n + 1$). The dependence $\Delta x = \Delta x(\Delta v)$ is depicted in Fig. 5, where we also discriminated between the interesting traffic states. The results clearly indicate that Δx is minimized if both cars move with the same velocity, irrespective of the microscopic state. Note that Δx is smaller than the mean distance derived from the inverse of the local density. Similar results and comparable conclusions were presented in [23], where the probability distribution $P(v_t - v_{t+\tau})$ was investigated. In this context v_t resp. $v_{t+\tau}$ are the speeds of two arbitrary (not necessarily consecutive) vehicles crossing the detector with a temporal distance of τ seconds. They also observed a

terized by a large value (≈ 1) of the cross-covariance between the local density and the local flow as defined by (3) and displayed in Fig. 11.

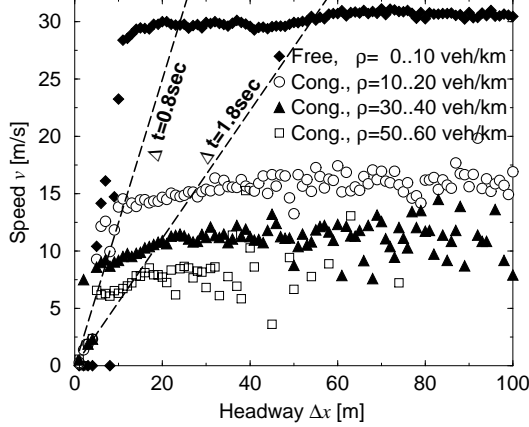


FIG. 4. The mean speed chosen by a driver depends on both the global traffic state and the gap to his predecessor. For a better orientation the regions of characteristic temporal headways are also displayed.

peak at $v_t - v_{t+\tau} = 0$ for any τ .

These observations are the motivation to determine an OV-function using exclusively the data where $|\Delta v_n| \leq 0.5 \text{ m/sec}$, because these should be relevant if an empirical OV-function is demanded as input parameter for traffic models. By using this reduced data set a better convergence of the OV-function in the high density regime is observable (Fig. 6). Nevertheless, at least the results in the free-flow and congested regime strongly differ. This indicates that in congested traffic the drivers do not only react on the distance to next vehicle ahead, they also take into account the situation at larger distances. It should be noticed that the dropping of measurements with $|\Delta v_i| > 0.5 \text{ m/sec}$ leaves only a fifth part of the data, but the quality of the OV-diagrams does not suffer very much from this restriction.

In order to give explicit measures for the OV-functions in the different density regimes we used the ansatz:

$$V(\Delta x) = k [\tanh(a(\Delta x - b)) + c] \quad (1)$$

suggested by Bando et al. [10], where a, b, c, k serve as fit parameters. In Fig. 7 the empirical relations $v = v(\Delta x)$ are displayed averaging (top) over all states corresponding to free-flow, (middle) over all congested states and (bottom) over all empirical data satisfying the restriction $|\Delta v| \leq 0.5 \text{ m/s}$. The comparison with an empirical OV-function established by analyses of a car-following experiment on a Japanese highway [10] reveals a higher value of $v(\infty)$ and a slower increase of the OV-function.

The characteristic values of the different OV-functions are summarized in Tab. I, where D denotes the distance where $V(D) = 0.95 \cdot V(\infty)$ holds. The numerical results show that when averaging over both free-flow and congested states (Fig. 7, bottom) the asymptotic regime of

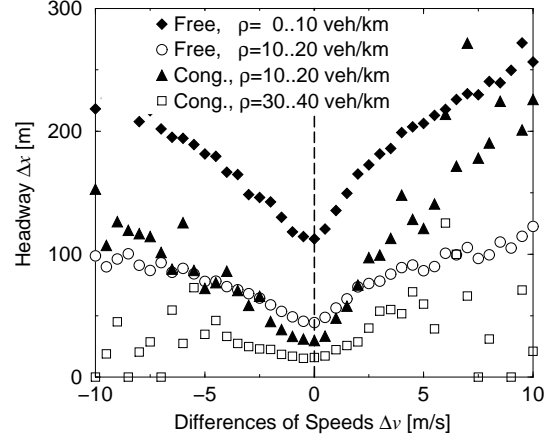


FIG. 5. The "driving comfort" is not decoupled from more "technical" features, i.e. vanishing differences of speed allow to drive at the smallest mean distance-headway.

the OV-function is reached at much larger distances.

	D	$V(\infty)$
Bando [10]	42.39	32.14
Free-flow (top)	14.11	29.43
Congested (middle)	26.70	11.47
All States (bottom)	57.70	28.64

TABLE I. Characteristic parameters of the OV-functions. The asymptotic values of the velocity $V(\infty)$ as well as the distance D where 95% of $V(D)$ are exceeded (refer to Fig. 7).

Our results for the OV-functions can be summarized as follows. In the free-flow regime the function are characterized by a steep increase at small distances corresponding to the small time-headways discussed in the previous subsection. For synchronized states it is remarkable that the asymptotic velocity takes a rather small value. Furthermore, our results show that it is necessary to distinguish between the traffic states in order to get a more precise description of the speed-headway relation.

IV. THE FUNDAMENTAL DIAGRAM

In this section we present results on the fundamental diagram based on time-averaged data. The present data set allows for a free choice of the averaging interval and overlaps. Here we compare the results obtained for one- and five-minute intervals. At the end of this section we discuss different methods in order to establish the stationary fundamental diagram. In Fig. 8 fundamental diagrams for averaging intervals Δt of one and five minutes

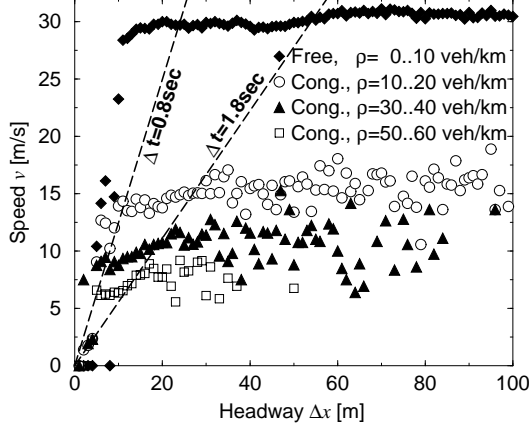


FIG. 6. If only vehicles with $|\Delta v_n| \leq 0.5 \text{ m/sec}$ are taken into account, the resulting OV-function differs slightly from Fig. 4. Especially in the congested states the measurements for $\Delta t \in [0.8 \text{ sec}, 1.8 \text{ sec}]$ are proportional to Δx , beyond $\Delta t = 1.8 \text{ sec}$ the data points are rather scattered.

are shown. Beyond the trivial effect that longer averaging intervals lead to a reduction of the fluctuations, one observes that both the extremal values of the density and the flow decrease with growing Δt . Moreover, the small flow values at very low densities are averaged out if five minute intervals are chosen. One might ask whether longer Δt 's hide some real structure of traffic states or whether the additional structure in the one minute intervals is a statistical artifact. From our point of view the results for the low density branch, which agree for both averaging intervals, indicate that a one-minute interval is sufficient to establish the systematic density dependence of the flow. Beyond that microscopic states with short lifetimes can be detected using short time-intervals which makes the one-minute intervals preferable.

The uncommon structure of the flow-density relation for small speeds, especially the return into the origin of the coordinate system, must be traced back to the method of the determination the local density via J/v , since the occupation itself was not accessible in the underlying data set. This behavior will be explained in more detail in Appendix A.

In order to obtain the *stationary* flow-density relationship we generated histograms from the fundamental diagram. Due to the problems of the density estimation in stop-and-go traffic we omit these states in the further discussion[§]. In Fig. 9 the results for two averaging procedures are displayed. The continuous form of the fun-

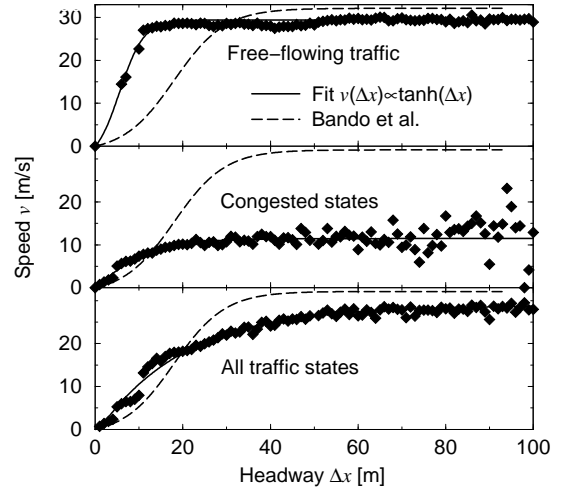


FIG. 7. Fits of the empirical data using the ansatz (1). The results are compared with the results given in [10]

damental diagram has been obtained by averaging over all flow values of a given density, while the discontinuous shape has been obtained discriminating between free-flow and congested traffic. It should be mentioned that the shape of the continuous stationary fundamental diagram also depends on the statistical weight of free-flow and congested states. Therefore from our point of view it is necessary to distinguish between the different states in order to obtain reasonable results for the stationary fundamental diagram.

Using the latter method it turns out that for high densities the average flow takes a constant value in a wide range of density. This plateau formation is similar to what is found in driven systems with so-called impurity sites or defects, where in a certain density regime the flow is limited by the capacity of the local defect [24–27]. Here the bottleneck effect is produced by lane-reduction as well as by the large activity of the on- and off-ramps at the intersection (see Section II).

V. TIME SERIES ANALYSIS

As already mentioned in the introduction we propose *objective* criteria for the classification of different traffic states using standard methods of time-series analysis. Beyond that we will show that these methods allow for a further characterization of the different states.

A. Auto-covariance function

The first quantity to consider is the auto-covariance

$$ac_x(\tau) = \frac{\langle x(t)x(t+\tau) \rangle - \langle x(t) \rangle^2}{\langle x^2(t) \rangle - \langle x(t) \rangle^2} \quad (2)$$

[§]See the following section for the identification of stop-and-go states.

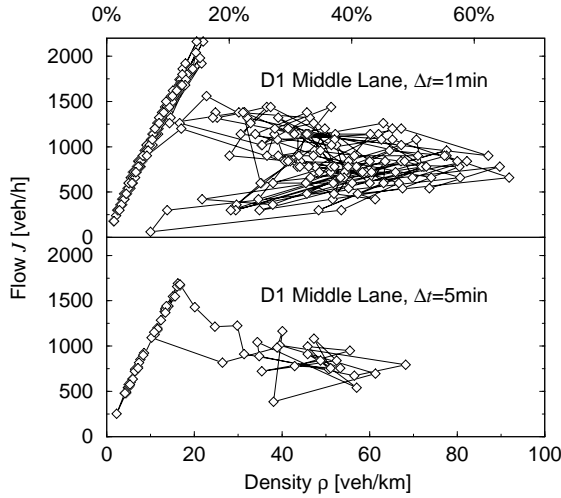


FIG. 8. Fundamental diagrams for different averaging intervals Δt . The upper diagram shows time-traced data averaged over $\Delta t = 1 \text{ min}$ while for the lower diagram $\Delta t = 5 \text{ min}$ has been used (for an explanation of the structure see also Appendix A and Fig. 16). The relative occupation is calculated using the maximal density during the measuring period, $\rho_{max} = 140 \text{ veh/km}$.

of the aggregated quantities $x(t)$. The brackets $\langle \dots \rangle$ indicate the average over a complete period of a free-flow or congested state. In Fig. 10 the auto-covariances of one-minute aggregates of the density, flow and average velocity of a free-flow and a congested state are shown. In the free-flow state the average speeds are only correlated on short time scales whereas long-ranged correlations are present in the time series of local density as well as of the flow. This implies that no systematic deviations of the average velocity from the constant average value are observable, while the density and therefore also the flow vary systematically on much longer time scales up to the order of magnitude of hours.

This behavior of the auto-covariance is clearly contrasted with the behavior found in synchronized traffic, where *all* temporal correlations are short-ranged irrespective of the chosen observable. Both results show that longer time scales are only apparent in slow variations of the density during a day, while the other time-series reveal a noisy behavior.

Furthermore, the cross-covariance

$$cc_{x,y}(\tau) = \frac{\langle x(t)y(t+\tau) \rangle - \langle x(t) \rangle \langle y(t+\tau) \rangle}{\sqrt{\langle x^2(t) \rangle - \langle x(t) \rangle^2} \sqrt{\langle y^2(t) \rangle - \langle y(t) \rangle^2}} \quad (3)$$

indicates the strong coupling between flow and density in the free-flow regime (Fig. 11). This implies that the variations of the flow are mainly controlled by density fluctuations while the average velocity is almost constant. Again the results for synchronized states differ strongly. Here all combinations of flow, density and average velocity lead to small values of the cross-covariance also sup-

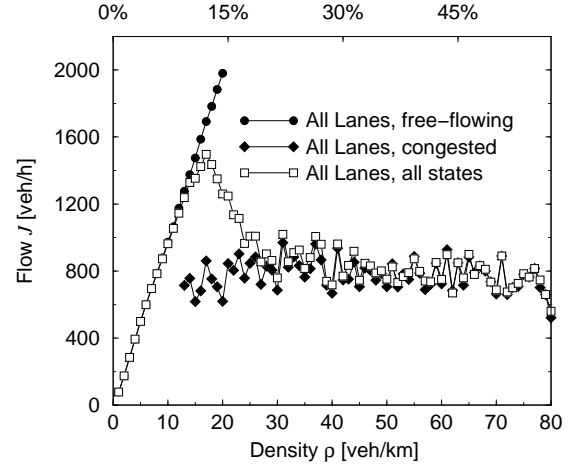


FIG. 9. Mean flow-density relation using the complete data set. The continuous curve corresponds to an average of all flow values for a given density while the discontinuous line is obtained discriminating between free-flow and congested states. Using the latter procedure a non-unique behavior of the flow-density relation is observable which can also be seen near local defects in driven systems. Data points of the congested branch have been dropped for low densities due to the unreliable statistics.

porting the existence of irregular patterns in the fundamental diagram. Therefore the covariance analysis of the empirical data are in agreement with the interpretation of empirical data given in [13,14], where synchronized states first have been identified. The synchronized states can be distinguished from stop-and-go traffic [15] using the same methods. Similar to free-flow states stop-and-go traffic is characterized by strong correlations between density and flow ($cc_{\rho,J}(0) \approx 1$). Beyond that also the auto-covariance function shows an interesting behavior namely an oscillating structure for all three quantities of interest. The period of these oscillations is given by $\approx 10 \text{ min}$. This result is in accordance with measurements by Kühne [28], who found oscillating structures in stop-and-go traffic with similar periods.

B. Transitions between the different states

These previous results show that the time-series analysis allows for an identification of different traffic states. Now we focus on the transition regime. Compared to the typical life-time of a free-flow or a congested state the transition is of short duration of approximately the order of magnitude of fifteen minutes (see Fig. 13 for a typical time-series of the local speed including a congested state).

Transitions from free-flow to both congested states are observable in the data set. The transitions take place at densities significantly lower than the density of maximum

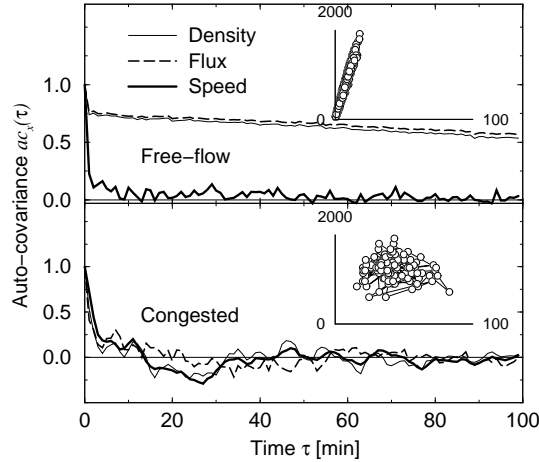


FIG. 10. Typical auto-covariance functions of the local density, the average velocity and the flow in a free-flow (top) and congested (bottom) state. The insets show the fundamental diagram corresponding to the chosen time-interval.

flow, since the transitions are initiated by a reduction of the capacity of the bottleneck and not by a continuous increase of the local density. We also want to mention that the congested states often are composed of stop-and-go and synchronized states, i.e. during a time-series corresponding to congested traffic frequently transitions between both congested states occur.

The results of several other empirical investigations suggest that the transition between free and congested flow is accompanied by a peak of the velocity variance at the transition [5,28,29]. Our analysis clearly does not support this result. The existence and height of the peak is closely related to the length of the averaging intervals. But of course these peaks are numerical artifacts. They show up because the time interval includes two different states but do not reflect any further characteristics of the transition.

C. Correlation between different lanes

In addition to the irregular pattern in the fundamental diagram it has been argued that a characteristic feature of the synchronized states is the strong coupling between different lanes [13,14]. These interpretations are mainly based on the fact that the average speeds on the different lanes approach each other. Here this effect is not observable because due to the speed-limit even in the free-flow regime the average velocities on different lanes only slightly differ (the average speed in the free-flow regime on the left lane is given by $\approx 120 \text{ km/h}$ and on the two other lanes by $\approx 100 \text{ km/h}$). Therefore we calculated $cc_{x_i, x_j}(\tau)$ in order to quantify this coupling effect. Here x_i denotes the flow, density, or speed on lane i . In

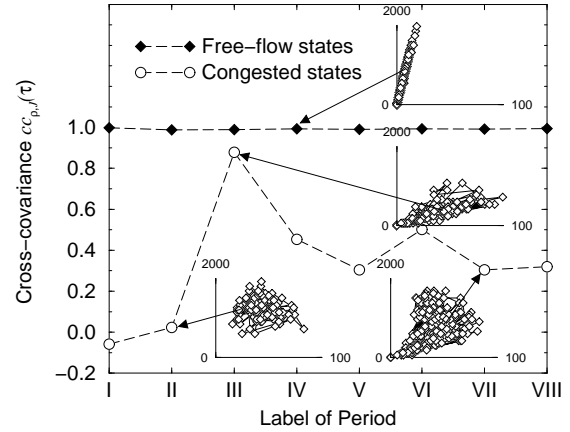


FIG. 11. Strong correlations between density and flow, indicated by $cc_{\rho,j}(0) \approx 1$, can be found in both free-flow and stop-and-go traffic. By contrast synchronized states are characterized by weak correlations between density and flow. Congested states where transitions between synchronized and stop-and-go traffic appear lead to intermediate values of $cc_{\rho,j}(0) \approx 0.2 \dots 0.5$. The different periods of free-flow and congested traffic are labeled by I through VIII (see also Section II). The dashed lines are a guide to the eyes only.

Fig. 14 the cross-covariances of different lanes belonging to the same driving direction are shown. The coupling between flow and density in the synchronized state is comparable to the free-flow state. It is also apparent that the free-flow signal is veritable on long time-scales, while in synchronized states the correlations rapidly decay with time. Again this result mainly reflects the daily variation of the density.

The synchronization of the different lanes is indicated by large value ($cc_{v_i, v_j}(0) \approx 0.9$) of the cross-covariance of the speed at $\tau = 0$, while the time series of the speed on different lanes in free-flow are completely decoupled.

D. Time-series of the single-vehicle data

In the previous section it could be shown that the relevant time-scales are identifiable by time-series analyses. Here these methods, in particular a generalization of the cross-covariance function, will be used in order gain further information on the different microscopic states.

By using the single-vehicle data directly it is not possible to evaluate the time-dependence of $ac_x(t)$ in realistic units because the time-intervals between consecutive signals strongly fluctuate. Instead of the temporal difference τ now the number of cars n passing the detector between vehicle i and $j = i + n$ is used.

The behavior of the auto-covariance in the free-flow regime can be characterized as follows. For small n 's one

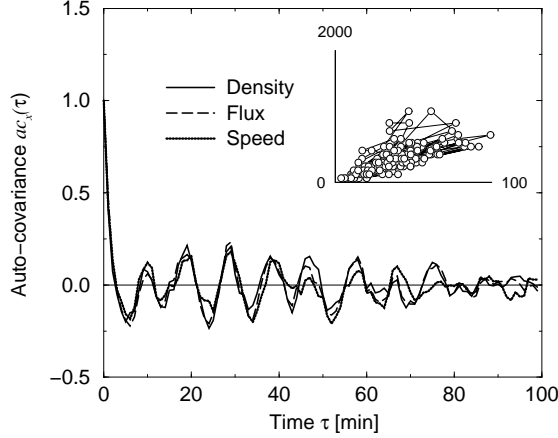


FIG. 12. The auto-covariances of all three local measures in stop-and-go traffic. All three local measures show oscillations around 0 with a period of ≈ 10 min.

observes a steep decrease of $ac_x(n)$ while asymptotically slow decrease is found. The crossover from a fast to a slow decay has been observed for a small number of cars ($n \approx 5$).

In the free-flow regime the single vehicle data basically support the results obtained for the aggregated data, namely a strong coupling between the temporal headways (the single-vehicle analogy of the flow: $J \propto \Delta t^{-1}$) and the distances (corresponding to the density: $\rho \propto \Delta x$). Moreover, the slow asymptotic decay is mainly due to the daily variation of the density. A different behavior has been found for $ac_v(n)$. First the decay for small n is not as fast as for the other signals and second the function decays faster asymptotically. The asymptotic behavior, in turn, is in accordance with the result drawn from aggregated data. But from our point of view the slower decrease for short distances is of special interest. It implies that also in the free flow regime small platoons of few cars moving with the same speed are formed. These platoons lead to the peak at $\Delta t = 0.8$ sec in the time-headway distribution.

Having Fig. 15 in mind $ac_x(n)$ of congested-state quantities behaves similarly, except for two differences: First of all no long-ranged signal is present for all quantities of interest and second the decay of $ac_v(n)$ for small n is much weaker than in the free-flow regime. This leads to the following picture of the microscopic states in synchronized flow: Similar to the free flow regime platoons are formed with cars moving at the same speed, but in synchronized flow these platoons are much larger (of the order of magnitude of some ten vehicles).

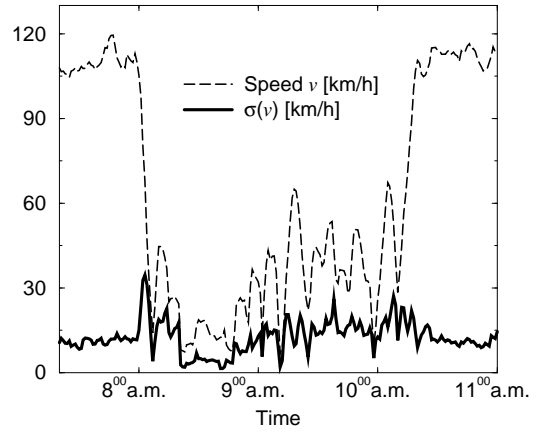
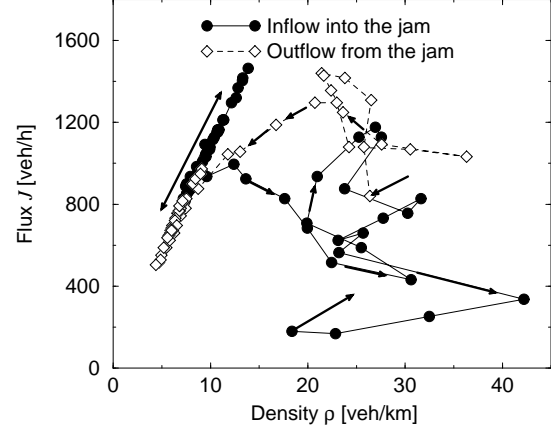


FIG. 13. Transitions between free-flow and congested traffic. The upper diagram shows one minute aggregates of the flow near a transition from free-flow to a congested state and vice versa. For comparison the time-series of the one-minute aggregates of the local speed and their standard deviations are given in the diagram below.

VI. SUMMARY AND CONCLUSION

In this paper a detailed statistical analysis of single-vehicle data of highway traffic is presented. The data allow to analyze the microscopic structure of different traffic states as well as a discussion of time-averaged data.

Using the single-vehicle data directly we calculated the time-headway distribution and the headway-dependence of the velocity. Both quantities are of great interest for modeling of traffic flow, because they can be directly compared with simulation results [17] or are even used as input parameters [10] for several models.

Our analysis of the time-headway distribution has revealed a qualitative difference between free-flow and synchronized states. The time-headway distribution of free-flow states shows a two-peak structure. The first peak

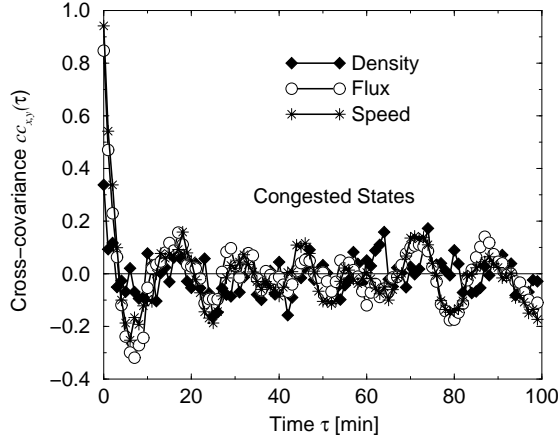
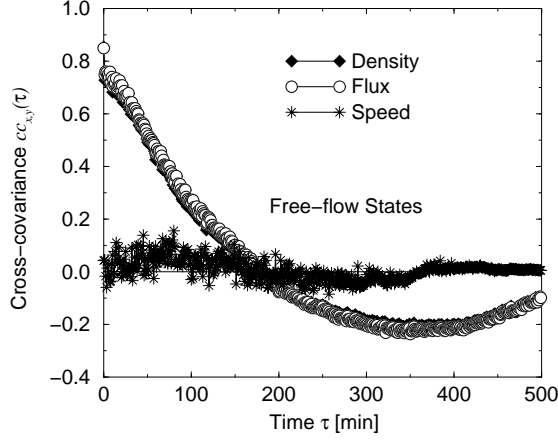


FIG. 14. Cross-covariance of flow, density and speed of different lanes in the free-flow regime compared to congested states.

is located at very small time-headways ($\Delta t \approx 0.8$ sec) while a second peak shows up at $\Delta t \approx 1.8$ sec. The second peak is also observed in congested flow but smaller time-headways are significantly reduced. The small time-headways correspond to very large values of the flow. Therefore the peak at small time-headways can be interpreted as a microscopic verification of meta-stable free-flow states.

Similar results have also been obtained for the speed distance relation, the so-called OV-function [10]. It also turned out that it is necessary to distinguish between free-flow and congested states. In particular the asymptotic velocities in free-flow and congested states differ strongly. Moreover a global average leads to different characteristics at small distances.

For comparison with earlier empirical investigations [13–15,29] we also have used aggregated data in order to calculate the fundamental diagram. Our results indicate that one minute intervals are preferable compared to

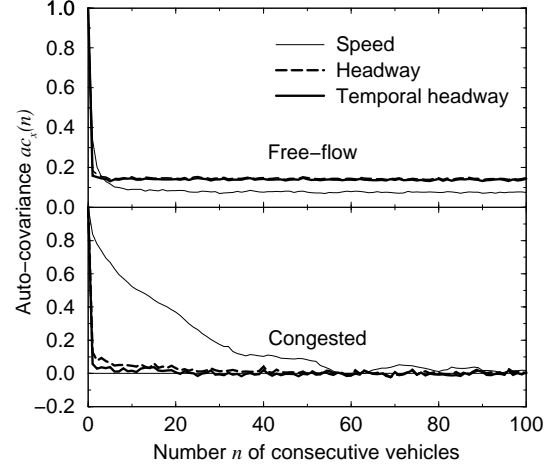


FIG. 15. A long-range signal is obtained from the auto-covariance of spatial and temporal headways among free-flowing vehicles (top). The diagram below is related to congested states and makes clear that the correlations of the speeds are large on short scales (up to 50 vehicles), whereas that of the spatial and temporal headway decays very abruptly.

five minute periods (see [5] for comparison) although this short intervals lead to larger fluctuations. Nevertheless, from our point of view, the single-vehicle data suggest that these fluctuations are not an artifact of the short averaging procedure but represent the complex structure of the different traffic states.

The data have also been used to calculate a stationary fundamental diagram. Again our results show that it is necessary to distinguish between free-flow and congested states in order to get reliable results for the average flow at a given density. Then one obtains a discontinuous form of the fundamental diagram and a non-unique behavior of the flow at low densities.

Using the auto-covariance function and cross-covariance for the different time-series we were able to identify three qualitatively different microscopic states of traffic flow, namely the free-flow, synchronized and stop-and-go traffic [20]. The free-flow states are characterized by a strong coupling of the flow and density and beyond that by a slow decay of the related auto-covariance functions. This implies that as far as a free-flow state is present the flow solely depends on the density. The time-scale which governs the asymptotic decay of the auto-covariance function is also determined by the daily variance of the density.

As shown in section II one can easily distinguish free-flow and congested-states. By contrast it is much more difficult to separate between time-series belonging to stop-and-go and synchronized states by inspection. Therefore an *objective* criterion is of great interest. It turns that the time-series analysis provides such crite-

tion. Synchronized states are indicated by small values of the cross-covariance between flow, speed and density. Moreover the auto-covariance function is short-ranged for all three quantities. These results reflect the completely irregular pattern in the flow density plane [13,14] found for synchronized states. By contrast, in stop-and-go traffic flow and density are strongly correlated. On the other hand, the auto-covariance function reveals an oscillating structure [28] with a period of the order of ten minutes. In addition it was found that transitions between free-flow and congested flow are rare but transitions between the different congested states are more frequent.

The auto-covariance functions of the single-vehicle data have suggest that in the free-flow regime as well as in synchronized states platoons of cars moving with the same velocity can be observed. Presumably the platoons in the free-flow regime lead to the peak at $\Delta t \approx 0.8$ in the time-headway distribution and therefore to very large values of the flow.

From our point of view our results have important implications for the theoretical description of traffic flow phenomena. The short distance-headways present in free-flow traffic are only possible when drivers anticipate the behavior of the vehicles in front of him [30]. Anticipation is less important in congested traffic. Another important effect is reflected by the gap-dependence of the velocity at high densities. Here we observe a small asymptotic velocity. This implies that drivers tend to hold their speed in dense states, another feature which has to be captured by traffic models. Finally, one has to take into account the reduced outflow from a jam which has been verified by other authors and is supported by our results.

In conclusion the analysis of single-vehicle data leads to a much better understanding of the microscopic structure of different traffic states. Although our results give a consistent picture of the experimental facts on highway traffic an enlarged data set or data from other detector locations would be very helpful in order to settle the experimental findings. First of all a series of counting loops would allow a more detailed analysis of the spatio-temporal structure of highway traffic, additional data from on- and off-ramps would help to discriminate between bulk and boundary effects.

APPENDIX A:

In principle one could use the single vehicle data directly in order to establish the velocity-flow relationship because the speed and the time-headway (which is proportional to the inverse flow) of individual cars are provided by the detector. Unfortunately, an interpretation of these results is difficult because of the extreme fluctuations of the experimental data. Therefore we used aggregated data in order to determine a fundamental diagram. In particular we show the flow-density relationship of one

and five minute aggregates.

While the local flow is directly given in the data set one has to calculate the temporally averaged local densities ρ at the detector because the coverage** of a detector is not provided here. The local density can be calculated via the relation

$$\rho = J/v, \quad (4)$$

where $J \propto N$ is closely related to the total number of cars N crossing the detector during the time interval $[t, t + \Delta t]$, and $v = \sum v_n(t)/N$ the average velocity of the cars. Note that both the velocity $v_n(t)$ of the individual cars and the flow J are directly accessible. Therefore this method should give the best estimate for the local density ρ as long as the velocity $v_n(t)$ represents a characteristic value of the local speed.

Problems using this kind of density calculation may arise from the strong fluctuations of the speed, especially in stop-and-go traffic. Then the velocity recorded by the detector gives a measure of the typical velocity of *moving* vehicles while the periods when cars do not move are not taken into account.

Fig. 16 illustrates the effect of the different measuring procedures using computer simulations. During the simulation of a continuous version of the NaSch-model (see Appendix B for a definition of the model) we used two kinds of detectors. The first detector is located at a link between two lattice sites. At this link we perform measurements of the number of passing cars (i.e. the local flow) and their velocity. Then the local density is calculated via (4). This result is compared with direct measurements of the local density where the average occupation on a short section of the lattice is detected. The figure shows that both estimates of the local density are in good agreement at low densities while at large densities the estimates may strongly differ. The different estimates for the local density lead to different shapes of the fundamental diagram. Estimating the density via the occupation of the detector we get the well known form of a high density branch while the calculation of the local density via (4) leads to a pattern which is similar to free-flow states but with a much smaller average velocity.

Similar patterns have also been found in our data set (see Fig. 8). Therefore the simulation results indicate that these periods correspond to stop-and-go traffic. Data points representing blocked cars are located in the origin of the fundamental diagram. Using a coverage-based density the points belonging to the same period would be shifted to the right. A deadlock situation would approach $(\rho_{max}, 0)$, with ρ_{max} the maximum density. We suppose that $\rho_{max} = 140 \text{ veh/km}$.

**The coverage of a detector denotes the fraction of time when the detector is occupied by vehicles.

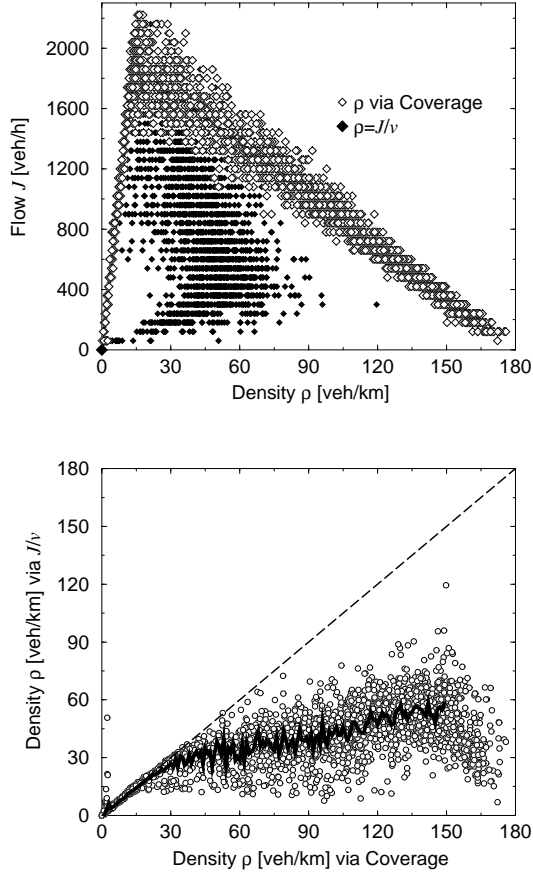


FIG. 16. Simulation results using different methods for the calculation of the local density. Top: The filled symbols correspond to an estimate calculated using (4), while the open symbols represent the coverage of the detector. Bottom: Comparison of both estimates. For $\rho > 30 \text{ veh/km}$ both methods strongly deviate from each other. Note that the density where these differences occur strongly depend on the chosen calibration of the model.

Finally we want to mention that this problem cannot be circumvented using the speed-flow relation because one is still left with the problem of overestimating local speeds in stop-and-go traffic.

APPENDIX B:

The simulation results have been obtained using a space-continuous version of the Nagel-Schreckenberg (NaSch) model [8] for single-lane traffic. Analogous to the NaSch model the velocity of the n -th car in the next time step is determined via the following four rules which are applied synchronously to all cars:

Step 1: Acceleration

$$V_n \rightarrow \min(V_n + 1, V_{\max})$$

Step 2: Deceleration (due to other vehicles)

$$V_n \rightarrow \min(V_n, d_n).$$

Step 3: Randomization

$$V_n \rightarrow \max(V_n - \text{rand}(), 0) \text{ with } \text{rand}() \in [0, 1]$$

Step 4: Movement

$$X_n \rightarrow X_n + V_n.$$

The velocity of the n -th car V_n is given in units of 5 m/s . V_{\max} denotes the maximum velocity, X_n the position of the cars, $d_n = X_{n+1} - X_n - 1$ the distance to the next car ahead. X_n and d_n are also given in units of 5 m (the length of the cars). $\text{rand}()$ is a random number between 0 and 1. In our simulation we use $V_{\max} = 8$ which corresponds to 40 m/s in realistic units.

The discrete NaSch model is also able to generate such fundamental diagrams, but with a worse resolution – the line of stop-and-go traffic has a rather steep slope. This is why we decided to use the continuous version of the NaSch model. Note that beside the better spatial resolution of the continuous version, no qualitative difference between the continuous and discrete version of the model have been found.

Acknowledgments: It is our pleasure to thank B.S. Kerner and D. Chowdhury for fruitful discussions. The authors are grateful to "Landschaftsverband Rheinland" (Cologne) for data support, to "Systemberatung Povse" (Herzogenrath) for technical assistance, to the Ministry of Economy, Technology and Traffic of North-Rhine Westfalia, and to the German Ministry of Education and Research for the financial support within the BMBF project "SANDY".

-
- [1] A. D. May, *Traffic Flow Fundamentals*, Prentice Hall, Englewood Cliffs (1990)
 - [2] C. F. Daganzo (Ed.): *Transportation and Traffic Theory*, Elsevier (1993)
 - [3] D.E. Wolf, M. Schreckenberg, A. Bachem (Eds.): *Traffic and Granular Flow*, World Scientific (1996)
 - [4] M. Schreckenberg, D.E. Wolf (Eds.): *Traffic and Granular Flow '97*, Springer (1998)
 - [5] D. Helbing, *Verkehrsdynamik*, Springer, Berlin (1998)
 - [6] M.J. Lighthill, and G.B. Whitham, Proc. Roy. Soc. A **229**, 317 (1955)
 - [7] R.E. Chandler, R. Herman, and E.W. Montroll, Op. Res. **6**, 165 (1958)
 - [8] K. Nagel, M. Schreckenberg, J. Physique I **2**, 2221 (1992)
 - [9] M. Schreckenberg, A. Schadschneider, K. Nagel, N. Ito, Phys. Rev. E **51**, 2939 (1995);
 - [10] M. Bando, K. Hasebe, A. Nakayama, A. Shibata, and Y. Sugiyama, Jap. J. Indust. Appl. Math. **11**, 203 (1994)
 - [11] M. Koshi, M. Iwasaki, and I. Okuhra, in *Proceedings of the 8th International Symposium on Transportation and Traffic Theory*, edited by V.F. Hurdle, E. Hauer, and

- G.N. Steward (University of Toronto Press, Toronto, Ontario 1983), p. 403
- [12] F.L. Hall, B.L. Allen and M.A. Gunter, Transp. Res. **A20**, 197 (1986)
 - [13] B.S. Kerner and H. Rehborn, Phys. Rev. E **53**, R4275 (1996)
 - [14] B.S. Kerner and H. Rehborn, Phys. Rev. Lett. **79**, 4030 (1998)
 - [15] B.S. Kerner, Phys. Rev. Lett. **81**, 3797 (1998)
 - [16] J. Treiterer: Ohio State Technical Report No. PB 246 094, (1975)
 - [17] D. Chowdhury, A. Majumdar, K. Ghosh, S. Sinha and R.B. Stinchcombe, Physica A **246**, 471 (1997)
 - [18] D. Chowdhury, L. Santen, A. Schadschneider, S. Sinha and A. Pasupathy, J. Phys. A **32**, 3229 (1999)
 - [19] A. Schadschneider, Eur. Phys. J. B (in press)
 - [20] B.S. Kerner, in [4]; p. 239
 - [21] R. Barlovic, L. Santen, A. Schadschneider and M. Schreckenberg, Eur. Phys. J. B **5**, 793 (1998)
 - [22] B.S. Kerner and P. Konhäuser, Phys. Rev. E **48**, R2335 (1993)
 - [23] P. Wagner, Z. Naturforsch. **52a**, 600 (1997)
 - [24] S.A. Janowsky and J.L. Lebowitz, Phys. Rev. A **45**, 618 (1992)
 - [25] G. Schütz, J. Stat. Phys. **71**, 471 (1993)
 - [26] Z. Csahok, T. Vicsek, J. Phys. A **27**, L591 (1994)
 - [27] D. Chowdhury, A. Pasupathy and S. Sinha, Euro. Phys. J. B **5**, 781 (1998)
 - [28] R.D. Kühne, in *Proceedings of the 10th International Symposium on Transportation and Traffic Theory*; edited by N.H. Gartner and N.H.M. Wilson (Elsevier, New York, 1987) p. 119
 - [29] D. Helbing, Phys. Rev. E **55**, R25 (1997)
 - [30] W. Knospe, L. Santen, A. Schadschneider and M. Schreckenberg, Physica A **265**, 614 (1999)